Arch. Metall. Mater., Vol. 61 (2016), No 1, p. 425–432

DOI: 10.1515/amm-2016-0078

T. RZYCHOŃ*#, B. DYBOWSKI*

THE INFLUENCE OF ALUMINUM ON THE MICROSTRUCTURE AND HARDNESS OF Mg-5Si-7Sn ALLOY

Magnesium alloys due the low density and good mechanical properties are mainly used in the automotive and aerospace industry. In recent years, magnesium alloys are extensively developed for use in high temperatures (above 120°C). Among these alloys, magnesium alloys containing tin and silicon have large possibilities of application due to the formation of thermally stable intermetallic Mg_2Sn and Mg_2Si. In this paper the influence of aluminum and heat treatment on the on the microstructure and hardness of Mg-7Sn-5Si alloy is reported. It was found that the microstructure of Mg-7Sn-5Si alloy consist of α-Mg solid solution, Mg_2Sn and Mg_2Si compounds. Addition of 2 wt% of Al to Mg-7Sn-5Si alloy causes the formation of Al_2Sn phase. Moreover, Al dissolves in the α-Mg solid solution. The solution heat-treatment of tested alloys at 500°C for 24 h causes the dissolve the Mg_2Sn phase in the α-Mg matrix and spheroidization of Mg_2Si compound. The Mg_2Si primary crystals are stable at solution temperature. After ageing treatment the precipitation process of equilibrium Mg_2Sn phase was found in both alloys. The addition of aluminum has a positive effect on the hardness of Mg-7Sn-5Si alloy. In case of Mg-5Si-7Sn-2Al alloy the highest hardness was obtained for sample aged for 148 h at 250°C (88 HV2), while in case of Al-free alloy the highest hardness is 70 HV for material aged for 148 h at 250°C.

Keywords: Cast Magnesium Alloys, Mg-Si alloys, Mg-Sn alloys, microstructure, precipitation hardening

1. Introduction

Magnesium alloys have been attracting attention as an important lightweight materials and are being utilized in the automobile and aerospace industries. Commercial cast magnesium alloys (AZ91, AM50, AM60) have limited application because of poor creep resistance and poor mechanical properties at elevated temperature of 120ºC. The cause of this phenomenon is a low-melting point $Mg_{17}Al_{12}$ phase located at the grain boundaries [1-3].

To increase the creep resistance of Mg-Al alloys, alloying elements are introduced, such as silicon, strontium, calcium and rare earth metals. In the last decade, a Al-free magnesium-alloy grades with high creep resistance have been developed, which can be used for components working at a temperature of up to 300°C. This group comprises the following alloys: Mg-Zn-RE, Mg-Y-Nd-Zr and Mg-Nd-Gd-Zr. These alloys have a very good thermal stability of the main strengthening phase at up to 250°C. However, the Mg-Y-Nd-Zr alloys have high associated cost due to the high cost of yttrium and the difficulties in casting. Therefore there is a need for an alternative alloy (Mg-Nd-Gd-Zr) which has similar properties to Mg-Y alloys, but with foundry handling and associated costs like non-yttrium containing alloys [4-7].

One possible way to increase the high-temperature mechanical properties of cast magnesium alloys at low manufacturing costs is the addition of silicon because the Mg_2Si phase exhibits a high melting temperature (1085°C), high hardness, low thermal coefficient and high elastic modulus [6,8]. Mg-Si alloys can be divided into two groups: hypoeutectic (below 1.45 at.% Si) and hypereutectic (above 1.45 at.% Si). Unfortunately, the as-cast hypereutectic alloys have a low mechanical properties due to the presence of primary Mg2Si compound which forms the large particles in the matrix [9-14]. In order to improve the mechanical properties the modified treatment can be used, however, the improvement of mechanical properties after modification is not impressive. Another way to increase the mechanical properties at ambient and elevated temperatures of hypereutectic Mg-Si alloys is addition of alloying elements that promotes the formation of fine precipitates strengthening of the matrix. One of these elements is tin, which is readily available and has a positive effect on the mechanical properties at ambient and elevated temperatures. The solubility of Sn in α-Mg solid solution drops sharply from 14.85 wt% at the eutectic transformation temperature 561°C to 0.45 wt% at 200°C. This provides a fundamental basis for improving the mechanical properties of these alloys through ageing [15]. After the heat treatment, thermally stable phase Mg2Sn is distributed homogeneously in the α-Mg matrix enhanced strength properties [16].

In this paper, the aluminum was added to Mg-5Si-7Sn alloy in order to strengthening of α-Mg solid solution and the influence of this element on the microstructure and hardness was investigated. Moreover, the ageing treatment was performed and the influence of the heat treatment parameters on the microstructure and hardness was reported.

* SILESIAN UNIVERSITY OF TECHNOLOGY, FACULTY OF MATERIAL SCIENCE AND METALLURGY, 40-019 KATOWICE, 8 KRASIŃSKIEGO STR., POLAND

Corresponding author: tomasz.rzychon@polsl.pl

2. Experimental method

Magnesium alloys containing silicon, tin and aluminum were prepared, and its composition was analyzed by X-ray fluorescence spectroscopy (Table 1). Commercially pure Mg (99.8%), Si (99.5%), Sn (99.4%) and Al (99.6%) were used. Melting of the alloys was performed by induction melting in an alumina crucible under the protection of an argon atmosphere. The melt was maintained at 800°C for 3 min then poured into sand moulds. The solution treatment was performed at 500°C for 24 hours in argon atmosphere and water quenched to room temperature. The ageing treatment was performed at temperatures in the range between 200°C and 250°C from 4 to 148 hours.

TABLE 1

Chemical composition of tested alloy (wt.%)

Alloy	Chemical composition, wt.%			
	Mg	Si	Sn	Al
Mg-5Si-7Sn	Balance	5.2	7.4	-
Mg-5Si-7Sn-2Al	Balance	5.2	7.1	1.8

The microstructure of the alloys was analyzed by light microscopy and scanning electron microscopy (SEM) using a FE SEM Hitachi S-3400 N scanning electron microscope. EDS analysis was performed at the acceleration voltage of 15 keV. Microstructure observations were performed on the samples etched in reagent containing 3 mL HNO_3 and 97 mL C_2H_5OH. The FEI Titan 83/300 transmission electron microscope (TEM) was also used to analyze the phase composition and chemical composition of the intermetallic phases. Thin foils were prepared by electrolytic polishing. The electrolyte composition was 5.3 g lithium chloride, 11.16 g magnesium perchlorate, 500 mL methanol, and 100 mL 2-butoxyethanol. Polishing was performed at -45°C and 20 V. XRD patterns were obtained with a JEOL JDX-7S diffractometer with a copper anode. Registration was performed by 0.02° stepwise regression for 2θ ranging from 10° to 90° 2θ. Phase identification was performed using the ICDD PDF-4+database. Hardness measurement were carried out on Vickers hardness tester (Duramin A5) at a load of 2 kg.

3. Results and discussion

3.1. Microstructure of as-cast alloys

Microstructure of as-cast Mg-5Si-7Sn alloy is composed of primary dendrites crystals, matrix, Chinese script particles and dark irregular phase (Fig. 1a). Moreover, the matrix is non-uniformly etched and darker areas are visible in the LM images. It is indicate on the microsegregation of alloying elements in the solid solution, what is characteristic feature of cast alloys.

XRD analysis has been performed in order to identification of phases occurring in the alloys. Fig. 2 shows X-ray diffraction pattern of Mg-5Si-7Sn alloy, in which the α-Mg, Mg_2Si and Mg_2Sn phases were clearly identified. In case of Mg-5Si-7Sn-2Al alloy, the α-Mg, Mg2Si and Mg2Sn were also unambiguously found (Fig. 3). Moreover, small diffraction lines belongs to Al2Sn compound are visible, however this identification is not clear due to low intensity and overlapping diffraction lines of this phase.

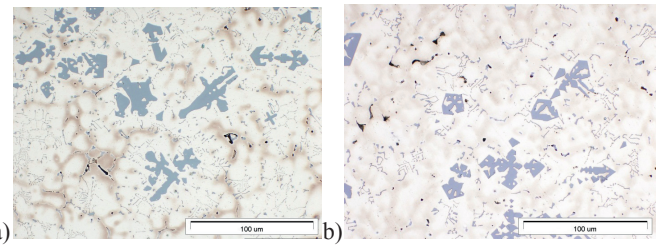

Fig. 1. LM images of tested alloys: Mg-5Si-7Sn (a), Mg-5Si-7Sn-2Al (b). Etching in solution of 3 % HNO_3 in ethanol

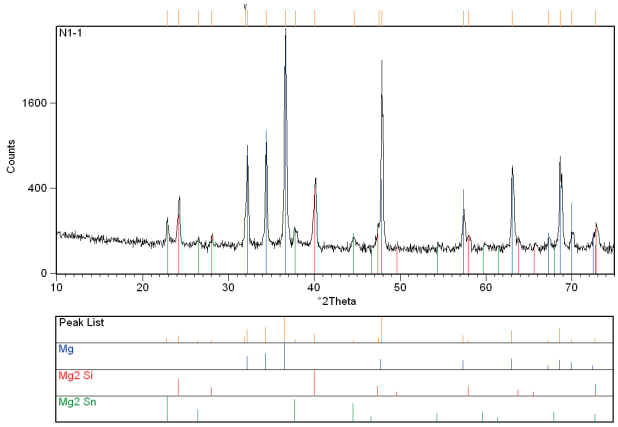

Fig. 2. X-ray diffraction pattern of Mg-5Si-7Sn alloy

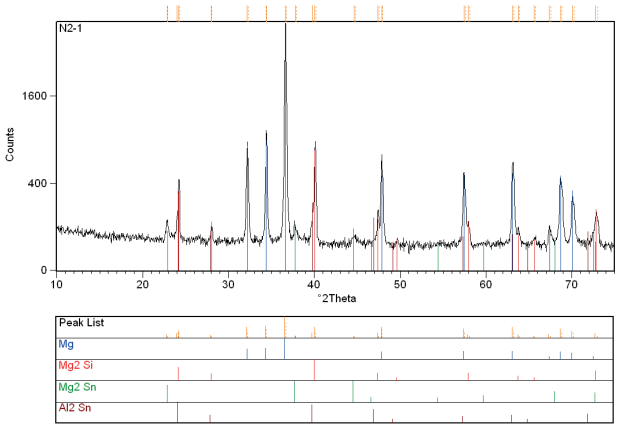

Fig. 3. X-ray diffraction pattern of Mg-5Si-7Sn-2Al alloy

Energy-dispersive spectroscopy (EDS) analysis was performed in order to identify the elemental composition of intermetallic phases and solid solution. Fig. 4 shows the SEM images of tested alloys with marked points correspond to sites of EDS microanalysis. The results of EDS analysis are shown in Table 2. Primary crystals (point 1) and Chinese script eutectic phase (point 2) are enriched in silicon, indicating the Mg_2Si phase. Minor amounts of Sn can dissolved in the Mg_2Si phase. The eutectic phase in point 3 (in the LM images this phase appears as dark phase) is mainly composed of magnesium and tin. Thus it can be concluded that it is the Mg_2Sn phase with solubility of silicon. In case of Mg_2Sn eutectic phase

appearing in the Mg-5Si-7Sn-2Al alloy (point 7) the EDS analysis revealed the presence of Al, which indicates that the Al dissolves in the Mg_2Sn phase. In the alloy with Al small particles consisting of aluminum and tin were found (point 5). Based on the XRD results it can be assumed that it is the Al_2Sn phase. Tin, besides the formation of the Mg_2Sn, dissolves in the α-Mg solid solution (points 4, 6). In the Mg-5Si-7Sn-2Al alloy, aluminum not only participates in the formation of the intermetallic Al2Sn phase, but also dissolved in the α-Mg matrix (about 1.2 at%).

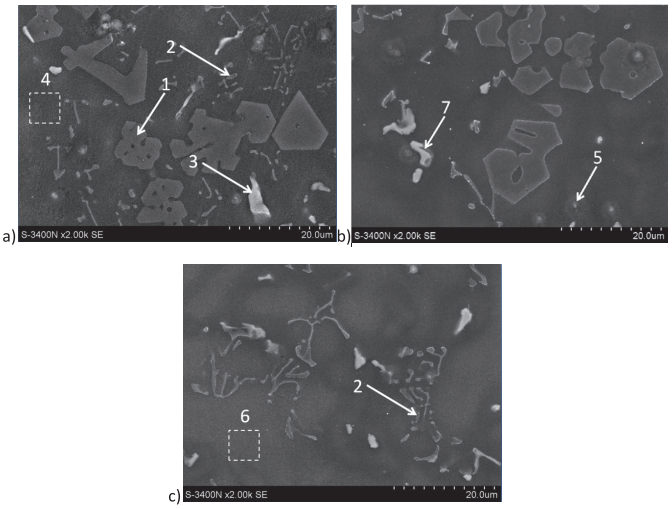

Fig. 4. SEM images of tested alloy with marked points of EDS analysis: Mg-5Si-7Sn (a), Mg-5Si-7Sn-2Al (b) and (c)

TABLE 2
Average (from points) the chemical composition of the phases in the as-cast alloys (at.%) using SEM/EDS

Point	Phase	Mg	Al	Si	Sn
1	Mg_2Si – primary crystals	65.6		33.3	1.1
2	Mg_2Si – Chinese script	92.0		6.5	1.4
3	Mg_2Sn in Mg-5Si-7Sn alloy	70.8		3.8	25.4
4	α-Mg in Mg-5Si-7Sn alloy	99.2			0.8
5	Al_2Sn (?)	89.5	6.9		3.6
6	α-Mg in Mg-5Si-7Sn-2Al alloy	96.3	1.2		0.9
7	Mg_2Sn in Mg-5Si-7Sn-2Al alloy	71.1	1.3	3.1	24.5

Considering the results obtained in this work, as well as results reported in [17] it can be concluded that the solidification sequence of Mg-5Si-7Sn and Mg-5Si-7Sn-2Al alloys begins with the nucleation of the primary Mg_2Si phase. With the decreasing melt temperature, Mg_2Si dendrites grow and the liquid phase surrounding them becomes enriched with Mg. When the local concentration is sufficient, the growth of Mg_2Si particles will be limited and Mg will nucleate on the Mg_2Si facets. Consequently, α-Mg halos surrounding Mg_2Si primary particles will be formed. Because the tin and silicon do not react with each other and no Si_xSn_y phases cannot be created in this alloy, two eutectic reaction should be appear during solidification: L → α-Mg + Mg2Si and L → α-Mg + Mg_2Sn. When the temperature of liquid metal reaches about 640°C the L → α-Mg + Mg_2Si reaction should occur. When the temperature will be close to 530°C, the eutectic consisting of α-Mg and Mg_2Sn phases will emerge. The excess of tin will dissolve in the α-Mg matrix due to high solubility Sn in Mg.

3.2. Microstructure of solution-treated alloys

Figure 5 shows a scanning electron micrograph of the solution treated alloys at 520°C for 24 h, from which it can be seen that microstructure of tested alloys is substantially altered. The Mg_2Sn compound in the both alloys have been dissolved into the magnesium matrix, due to high solubility of tin in magnesium (3.35 at.%) [18]. Primary crystals of Mg_2Si phase (point 2, Fig. 5, Table 3) have not been dissolved in the matrix of alloys and its chemical composition is close to its composition in as-cast state. The Mg_2Si phase with Chinese script morphology, which is formed as a result of eutectic reaction at ~640°C, is also not dissolved in the α-Mg matrix. The Mg_2Si phase have not been dissolved in the α-Mg solid solution due to the very low solubility of silicon in magnesium (0.005 at.%). It is noteworthy that the stability of the Mg_2Si eutectic compound is much less than the stability of Mg_2Si primary crystals at solution temperature (500°C) and the spheroidization of Chinese script particles is observed (point 3, Fig. 5, Table 3). Because the solubility of Si in Mg is close to zero, the diffusion of atoms occurring at the Mg/Mg_2Si interface. It is well known that particle size, especially particles radius (Gibbs-Thomson equation), has an influence on their tendency to the form the spherical shape. Therefore, the spheroidization process of the Mg_2Si eutectic compound is related to smaller size of Chinese particles in comparison to primary crystals of Mg_2Si. Microstructure observation indicates that the Al_2Sn compound remain stable after the solution heat treatment due to high melting point of this phase.

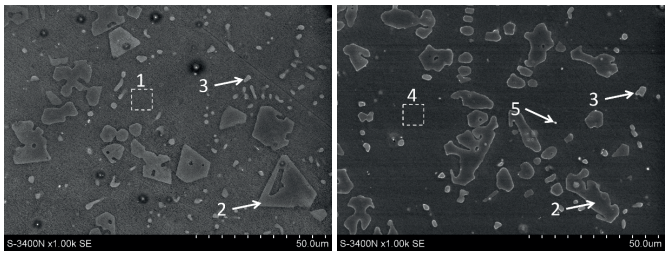

Fig. 5. SEM image of solution-treated Mg-5Si-7Sn alloy (a) and Mg-5Si-7Sn-2Al alloy (b) and EDS results from points marked in the Figures

TABLE 3
Average (from 5 points) the chemical composition of the phases in the solution-treated alloys (at.%) using SEM/EDS

Point	Phase	Mg	Si	Al	Sn
1	α-Mg in Mg-5Si-7Sn alloy	98.1			1.9
2	Mg_2Si – primary crystals	64.8	33.9		1.2
3	Mg_2Si – globular	81.7	16.3		1.9
4	α-Mg in Mg-5Si-7Sn-2Al alloy	96.9		1.7	1.4
5	Al_2Sn (?)	86.1	0.5	5.8	7.6

The results of microstructural observations are further confirmed by the X-ray diffraction analysis, which can be seen in the Figures 6 and 7. The diffraction lines of α-Mg are shifted

towards higher angles compared to as-cast state. It is indicate a change the lattice parameters of α-Mg solid solution which are caused by the presence of tin atoms in the α-Mg matrix. The diffraction lines of Mg_2Sn compound are not observed due to the dissolution of Mg_2Sn phase in the solid solution. Because the Mg_2Si phase did not dissolve during the solution treatment at 500°C, its diffraction peaks are still visible in the X-ray diffraction pattern. As mentioned above, identification of Al_2Sn phase in as-cast Mg-5Si-7Sn-2Al alloy is ambiguous. In the solution-treated Mg-5Si-7Sn-2Al alloy diffraction lines belongs to Al_2Sn phase were not detected. However, it is not indicate its absence in the alloy due to minor content and overlapping of the strong diffraction lines with peaks of Mg_2Si compound.

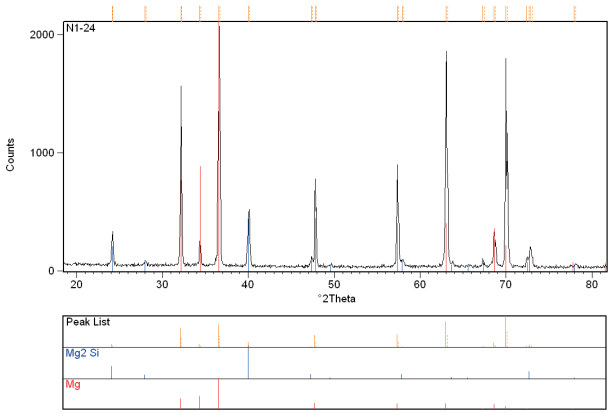

Fig. 6. X-ray diffraction pattern of solution-treated Mg-5Si-7Sn alloy

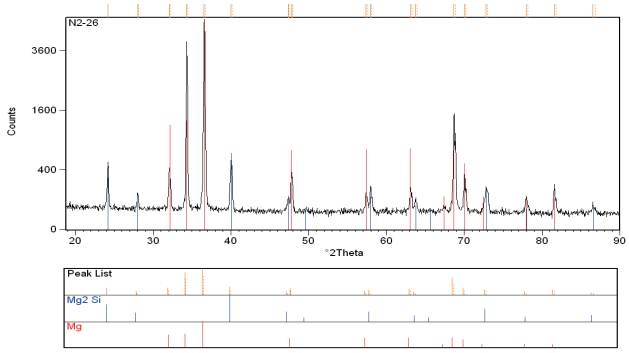

Fig. 7. X-ray diffraction pattern of solution-treated Mg-5Si-7Sn-2Al alloy

3.3. Microstructure of aged Mg-5Si-7Sn and Mg-5Si-7Sn-2Al alloys

Fig. 8 shows X-ray diffraction patterns of Mg-5Si-7Sn alloy aged at 250°C. From these results it can be seen that the Mg_2Sn phase precipitates in early stages of ageing. Moreover, the intensities of diffraction peaks of the Mg_2Sn phase increase with ageing time. It is indicate an increase the content of Mg_2Sn phase after the subsequent steps of ageing. Similar results were obtained for Mg-5Si-7Sn alloy aged at 200°C and Mg-5Si-7Sn-2Al aged at 200°C and 250°C. In binary Mg-Sn alloys the formation of Mg_2Sn phase is not preceded by the formation of intermediate phases (G-P zones, non-equilibrium compounds) [19]. Also in our case non-equilibrium phases were not observed and the precipitation process begins with the formation equilibrium Mg_2Sn phase.

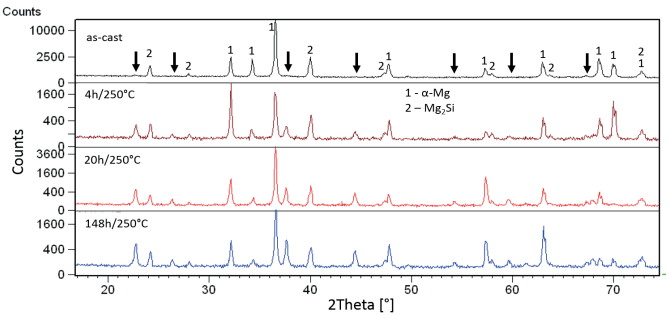

Fig. 8. X-ray diffraction patterns of Mg-5Si-7Sn alloy aged at 250°C

Figure 9a shows the a bright-field image of a typical microstructure of Mg-5Si-7Sn alloy aged at 250°C for 20 h. It can be seen that the Mg_2Sn phase precipitating during ageing treatment have the mainly rod-shaped morphology. The FFT pattern (Fig. 9d) confirms that the rod-shaped precipitates has the Mg_2Sn cubic crystal structure. Moreover, the plate-shaped precipitates of Mg_2Sn compound are visible in the α-Mg matrix in both alloys (Fig. 10). Microscopic observations using electron transmission microscopy suggest that the content of plate-shaped precipitates of Mg_2Sn phase is higher for alloy with aluminum, if compared with the alloy without aluminum. However, it should be emphasized that the volume fraction of plate-shaped precipitates has not been determined by a quantitative method and detailed results will be published later. The observations in dark-field image (Fig. 10b) show that the rod-shaped and plate-shaped precipitates of Mg_2Sn are bright, thus it can be concluded that these precipitates have the same orientation relationship with the α-Mg solid solution. Because this image was registered along the [0001] zone axis of α-Mg matrix, thus it can be stated that the Mg2Sn precipitates with two morphologies are mainly distributed on the {0001} basal plane of α-Mg phase. Obviously, the rod-shaped precipitates are visible not only on the basal planes, but also on non-basal planes, as shown in Fig. 9. Detailed results describing the orientation relationship between the Mg2Sn and α-Mg phase will be published later.

Fig. 11 shows a typical microstructure of both alloys after ageing treatment at 250°C for 148 h. The fine particles of Mg_2Sn phase are uniformly distributed in the α-Mg matrix. Moreover, the globular Mg_2Si phase is also visible in Fig. 12. The quantitative characterization of Mg_2Sn phase was also carried out (Table 4), from which it can be seen that the number of Mg_2Sn particles per unit area (NA) in Mg-5Si-7Sn-2Al alloy is slightly higher and the precipitates of Mg_2Sn compound in Mg-5Si-7Sn-2Al alloy have a slightly shorter length and slightly higher the number of Mg_2Sn particles. From Table 4 it can be seen that the differences are not too high, therefore two-sample t-test (test for the difference between two means) with significance level of 0.05 was performed. Because the P-values for NA and length of Mg_2Sn precipitates are higher than significance level, it can be stated that there is no significant difference between the NA and length of Mg_2Sn precipitates in these two alloys.

The primary crystals of Mg_2Si phase and globular particles of Mg_2Si phase are still visible in the microstructure of aged alloy due to their high thermal stability. There were no changes in the chemical composition and morphology of these phases.

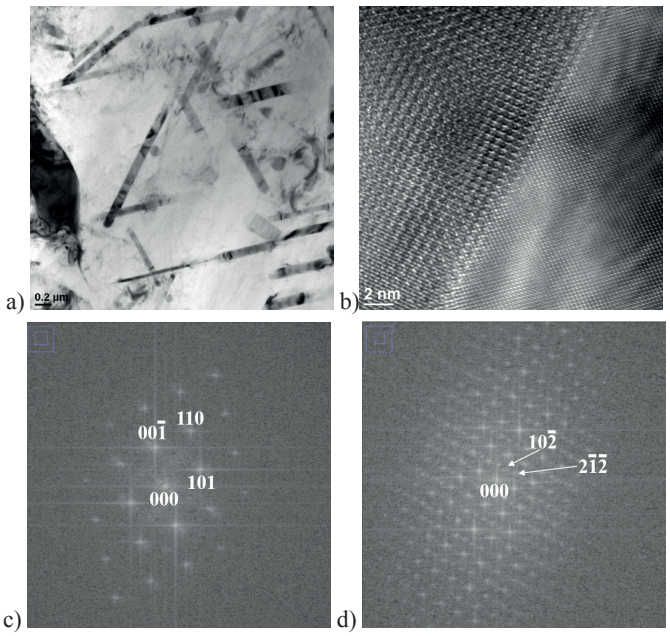

Fig. 9. The rod-shaped of Mg_2Sn precipitates observed in the Mg-5Si-7Sn alloy aged at 250°C for 20 h (a), HRTEM image of the interface between the Mg_2Sn precipitates and the α-Mg phase (b), FFT pattern from the α-Mg matrix, [-1101] zone axis (c), FFT pattern from the rod-shaped of Mg_2Sn precipitates, [221] zone axis (d)

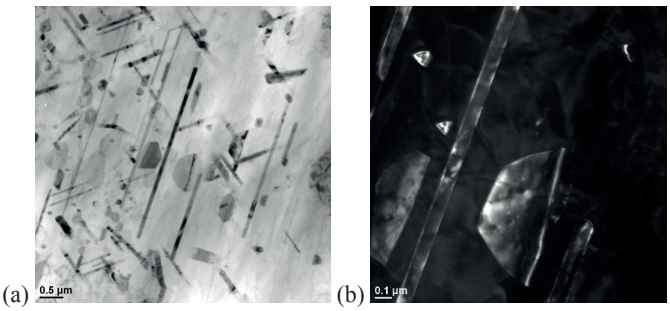

Fig. 10. The rod-shaped and plate-shaped of Mg_2Sn precipitates observed in the Mg-5Si-7Sn-2Al alloy aged at 250°C for 20 h (a), dark field image of plate- and rod-shaped Mg_2Sn precipitates in the alloy aged at 250°C for 20 h (b). TEM micrographs were obtained in the [0001]Mg beam direction. The chemical composition of rod-shaped precipitates is 77.3Mg-20.8Sn-1.9Al (at.%) - TEM/EDS analysis

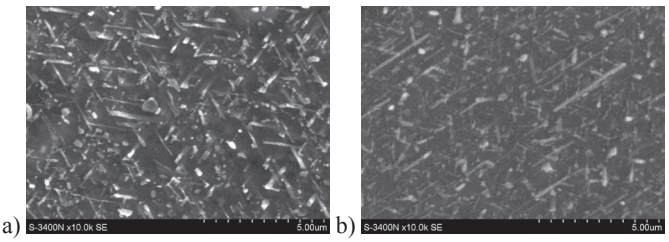

Fig. 11. SEM micrographs of Mg-5Si-7Sn (a) and Mg-5Si-7Sn-2Al (c) alloys aged at 250°C for 148 h with the precipitates of Mg_2Sn phase

TABLE 4
The results of quantitative characterization of Mg_2Sn phase in tested alloys aged at 250°C for 148 h

Point	N_A [1/m^2]	length l (µm)
Mg-5Si-7Sn	$4.8 \cdot 10^{12}$	1.02±0.31
Mg-5Si-7Sn-2Al	$5.12 \cdot 10^{12}$	0.87±0.70

3.4. Hardness of heat-treated Mg-5Si-7Sn and Mg-5Si-7Sn-2Al alloys

The hardness of as-cast Mg-5Si-7Sn alloy is 60 HV2, while the hardness of alloy with aluminum addition is 71 HV2. The content of Mg_2Si and Mg_2Sn compounds in both alloys is comparable, therefore the higher hardness of Mg-5Si-7Sn-2Al is attributed to the presence of Al solute atoms in α-Mg solid solution. Al has a great contribution to the solid-solution strengthening and belongs to the most efficient solid-solution strengthener for Mg due to large atomic size misfit (11 %) and high solubility in Mg at ambient temperature [20]. In previous studies [21], it was found that the increasing the Al solute content in α-Mg phase from 1.5 at. % to 2.9 at.% causes increase of α-Mg hardness from 45 to 53 HV. However, it should be not, that the increase in the hardness of Mg-5Si-7Sn-2Al alloy by 11 units of HV, which arises only from solid-solution strengthening by Al, it seems to be too high. Probably, the additional effect on the hardness also have a fine precipitates of Al_2Sn phase, however their content in Mg-5Si-7Sn-2Al alloy is low.

In the binary Mg-Sn alloys the solution heat treatment causes a reduction in hardness due to the dissolution of Mg_2Sn phase and α-Mg grain growth [22]. The solution heat-treatment at 500°C did not change the hardness of Mg-5Si-7Sn alloy (60 HV). Lack of changes in hardness of Mg-5Si-7Sn alloy is due to the presence of hard Mg_2Si primary crystals, which are stable after solution heat treatment. Thus, the dissolution of Mg2Sn phase in the matrix and spheroidization of eutectic Mg2Si phase did not result in decreasing the hardness. In case of Mg-5Si-7Sn-2Al alloy the hardness decreased slightly from 71 HV to 67 HV. From the obtained results it is difficult to deduce why the hardness of Mg-5Si-7Sn-2Al alloy is slightly decreased. Presumable, the raised Al content in α-Mg resulting from the dissolution of Mg_2Sn phase (Table 2 and Table 3) may exert the effect on the hardness. However, this explanation requires further detailed study.

Figure 12 shows the variation in Vickers hardness as a function of aging time at 200°C and 250°C. It can be seen that hardness of tested alloys increases with the increasing aging time. The age hardening behavior of tested alloys indicates that the aluminum addition enhance the hardness of Mg-5Si-7Sn alloy. In case of Mg-5Si-7Sn-2Al alloy the highest hardness was obtained for sample aged for 148 h at 250°C (88 HV2), while in case of Al-free alloy the highest hardness is 70 HV for material aged for 148 h at 250°C (70 HV2). Moreover, the hardness increment is significantly higher in alloy with aluminum. The hardness of Mg-5Si-7Sn-2Al alloy after 4 h of ageing is 81 HV (growth 14HV), whereas in Mg-5Si-7Sn alloy is 65 HV (growth 5HV). Thus, it can be concluded that aluminum addition causes a significant increase the hardness increment and hardness of Mg-5Si-7Sn alloy.

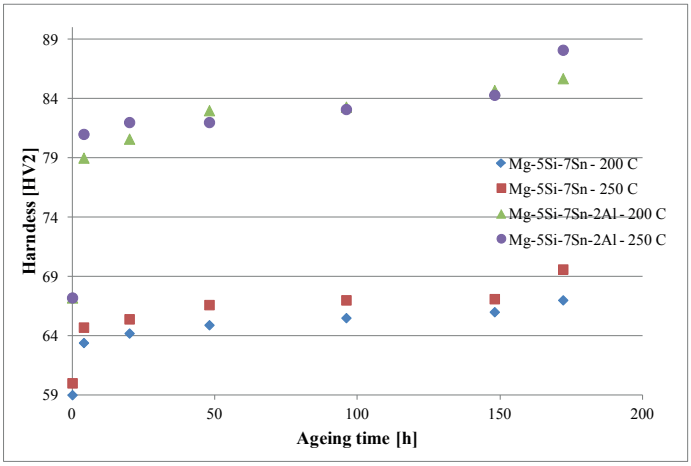

Fig. 12. The hardness of Mg-5Si-7Sn and Mg-5Si-7Sn-2Al alloys as a function of ageing time at 200°C and 250°C

It is well known that the age-hardening response in Mg-Sn alloy is only modest, despite the large content of Mg_2Sn precipitates that may be formed [23]. Also in Mg-5Si-7Sn alloy age-hardening response and hardness increment is only ≈ 10 HV. The reason for the poor precipitate strengthening response is that the precipitates form, in a relatively coarse distribution, with a rod-shaped morphology parallel to the basal planes of the Mg matrix. This configuration is relatively inefficient at impeding dislocation motion in the α-Mg matrix [23]. Microscopic observations performed in our work also suggests that the Mg_2Sn precipitates are parallel to the basal planes of the matrix, thus the hardness increment after ageing is relatively poor. Addition of aluminum causes a significant increase in the hardness of Mg-5Si-7Sn alloy. Al atoms may cause a solute-drag like effect for the Mg/Mg_2Sn interfaces, therefore the growth of the Mg_2Sn particles is hindered. It is well known that the finer size of precipitates and their higher number effectively strengthen the metallic alloys due to smaller average interparticle spacing and increased number of obstacles to movement of dislocations, thus the smaller length l and higher the number of Mg_2Sn particles per unit NA area should cause the hardness increment. The quantitative assessment of the Mg_2Sn precipitates (Table 4) showed that the precipitates in Al-rich alloy are slightly finer. However, these results do not allow for a clear explanation whether rod- and plate-shaped precipitates have a strong influence on the increase in the hardness, because the differences in the size and density of precipitates in these alloys are statistically insignificant.

Sasaki et al [22] and Mendis et al. [23] reported that the increase the hardness of Mg-Sn base alloy is related to formation of precipitates on non-basal crystallographic planes of α-Mg phase. Therefore, another possibility to increase the hardness of alloy with aluminum is present the Mg_2Sn precipitates on the pyramidal and prismatic planes. In this work, detailed studies concerning the orientation relationship between the Mg_2Sn and α-Mg phases were not performed, thus it has not been established whether the volume fraction of Mg_2Sn precipitates lying on the non-basal planes is higher in the Mg-5Si-7Sn-2Al alloy compared to the Al-free alloy.

In aged Mg-5Si-7Sn-2Al alloy any additional phases with aluminum, especially the $Mg_{17}Al_{12}$ phase, were not found in the microstructure. Only minor content of the Al_2Sn compound was observed (this compound was also present in as-cast alloy). In the solution heat-treated alloy the content of aluminum in the α-Mg matrix is about of 1.7 at.% (Table 3) which is less than the maximum solubility of Al in Mg at 250°C (ca. 3.5 at%), therefore precipitation of the $Mg_{17}Al_{12}$ phase should not occur during ageing at 250°C [24]. Thus, there are two possibilities: (i) Al remains in the α-Mg solid solution after ageing, (ii) Al atoms are located in the crystal lattice of Mg_2Sn phase, which is formed during the ageing treatment. In the first case (i) it should be noted that Al belongs to the most efficient solid-solution strengthener for Mg due to large atomic size misfit, therefore the higher hardness of Mg-5Si-7Sn-2Al alloy compared to Mg-5Si-7Sn alloy may be the result of the solid-solution strengthening. It seems unlikely due to the very large the hardness increment in the early stages of ageing (Fig. 12). It is more likely that the aluminum dissolves in the Mg_2Sn phase (ii). From the results analysis for as-cast alloys it can be assumed that the solubility of Al in Mg_2Sn compound is about of 1.5 at.%. In the aged Al-rich alloy aluminum also was found in the rod-shaped precipitates of Mg_2Sn phase, therefore the precipitation process in the alloy with aluminum is more effective and hardness increment is significantly higher.

Generally, the increase in hardness up to 88 HV2 for Mg-5Si-7Sn-2Al alloy aged at 250°C for 148 h is attributed to presence of aluminum in the Mg_2Sn phase. It cannot be excluded that the influence on the hardness exert the presence Al atoms in the α-Mg solid solution and formation of Mg_2Sn precipitates on the non-basal planes. However, the detailed effect of individual factors requires additional studies.

4. Conclusions

The microstructure as-cast Mg-5Si-7Sn alloy is composed of α-Mg solid solution, primary dendrites crystals of Mg_2Si phase, Chinese script Mg_2Si phase, and irregular Mg_2Sn phase. Addition of aluminum to Mg-5Si-7Sn alloy results in the formation of Al_2Sn phase and dissolution of Al in α-Mg matrix. The solution heat-treatment of tested alloys at 500°C for 24 h causes the dissolve the Mg_2Sn phase in the α-Mg matrix and spheroidization of Chinese script Mg_2Si compound. The Mg2Si primary crystals are stable at solution temperature. After ageing treatment the precipitation process of rod- and plate-shaped equilibrium Mg_2Sn phase was found in both alloys. The Mg_2Sn precipitates with two morphologies are mainly distributed on the {0001} basal plane of α-Mg phase. The hardness of as-cast Mg-5Si-7Sn alloy is 60 HV2, while the hardness of alloy with aluminum addition is 71 HV2. The solution heat-treatment at 500°C did not change the hardness of Mg-5Si-7Sn alloy (60 HV). In case of Mg-5Si-7Sn-2Al alloy the hardness decreased slightly from 71 HV to 67 HV. The hardness of tested alloys increases with the increasing aging time. In case of Mg-5Si-7Sn-2Al alloy the highest hardness was obtained for sample aged for 148 h at 250°C (88 HV2), while in case of Al-free alloy the highest hardness is 70 HV for material aged for 148 h at 250°C. The hardness increment is significantly higher in alloy with aluminum.

Acknowledgments

The present work was supported by the National Science Centre under the project UMO-2011/03/D/ST8/03869. The author is grateful to P. Skupień (IMŻ Gliwice) for their assistance.

REFERENCES

[1] H. Friedrich, B.L. Mordike, Magnesium Technology, Berlin 2006.
[2] A.A. Luo, Int. Mater. Reviews **49**, (1), 13-30 (2004).
[3] K.N. Braszczyńska-Malik, J. Alloys Compd. **477**, 870-876 (2009).
[4] B. Dybowski, A. Kiełbus, R. Jarosz, J. Paśko, Solid State Phenom. **211**, 65-70 (2013).
[5] B. Płonka, J. Kut, P. Korczak, M. Lech-Grega, M. Rajda, Arch. Metall. Mater. **57**, (2), 619-626 (2012).
[6] F. Mirshahi, M. Meratian, Mater. Des. **33**, 557-562 (2012).
[7] T. Rzychoń, J. Szala, A. Kiełbus, Arch. Metall. Mater. **57**, (1), 245-252 (2012).
[8] N. Zheng, H.Y. Wang, Z.H. Gu, W. Wang, Q.C. Jiang, J. Alloys Compd. **463**, L1-L4 (2008).
[9] L. Wang, E. Guo, B. Ma, J. Rare Earth **26**, 105-109 (2008).
[10] Q.C. Jiang, H.Y. Wang, Y. Wang, B.X. Ma, J.G. Wang, Mater. Sci. Eng. A **392**, 130-135 (2005).
[11] Q.D. Qin, Y.G. Zhao, C. Liu, P.J. Cong, W. Zhou, J. Alloys Compd. **454**, 142-146 (2008).
[12] H.Y. Wang, Q.C. Jiang, B.X. Ma, Y. Wang, J.G. Wang, J.B. Li, J. Alloy Compd. **387**, 105-108 (2005).
[13] M. Yang, F. Pan, J. Liang Bai, Trans. Nonferr. Metal. Soc. China **19**, 287-292 (2009).
[14] E.J. Guo, B.X. Ma, L.P. Wang, J. Mater. Process. Technol. **206**, 161-166 (2008).
[15] H. Liu, Y. Chen, Y. Tang, D. Huang, G. Niu, Mater. Sci. Eng. A **437**, 348-355 (2006).
[16] G. Nayyeri, R. Mahmudi, Mater. Sci. Eng. **A 527**, 4613-4618 (2010).
[17] Y. Pan, X. Liu, H. Yang, Mater. Charact. **55**, 241-247 (2005).
[18] A.A. Nayeb-Hashemi, J.B. Clark, Bull. Alloy Phase Diagrams, **5**, 466-475 (1984).
[19] M.A. Gibson, X. Fang, C.J. Bettles, C.R. Hutchinson, Scripta Mater. **63**, 899-902 (2010).
[20] A. Suzuki, N.D. Saddock, I. Riester, E. Lara-Curzio, J.W. Jones, T.M. Pollock, Metall. Mater. Trans. A, **38A**, 420-427 (2007).
[21] T. Rzychoń, B. Adamczyk-Cieślak, Arch. Metall. Mater. **59**, (1), 329-334 (2014).
[22] T.T. Sasaki, J.D. Ju, K. Honoa, K.S. Shinb, Scripta Mater. **61**, 80-83 (2009).
[23] C.L. Mendis, C.J. Bettles, M.A. Gibson, C.R. Hutchinson, Mater. Sci. Eng. A, **435–436**, 163-171 (2006).
[24] T. Rzychoń, A. Kiełbus, L. Lityńska-Dobrzyńska, Mater. Charact. **83**, 21-34 (2013).

Received: 20 march 2015